Review

Alternatives for Connecting Photovoltaic Generators to Power Systems with Three-Port and Partial Power Converters

Donghui Ye and Sergio Martinez *

Department of Electrical Engineering, Escuela Técnica Superior de Ingenieros Industriales,
Universidad Politécnica de Madrid, 28006 Madrid, Spain; donghui.ye@alumnos.upm.es
* Correspondence: sergio.martinez@upm.es

Abstract: Solar electricity has become one of the most important renewable power sources due to rapid developments in the manufacturing of photovoltaic (PV) cells and power electronic techniques as well as the consciousness of environmental protection. In general, PV panels are connected to DC-DC converters and/or DC-AC inverters to implement the maximum power point tracking algorithm and to fulfill the load requirements. Thus, power conversion efficiency and power density need to be taken into consideration when designing PV systems. Three-port and partial power conversion technologies are proposed to improve the efficiency of a whole PV system and its power density. In this paper, three types of three-port converters (TPCs), including fully isolated, partly isolated, and non-isolated TPCs, are studied with detailed discussions of advantages, disadvantages, and comparisons. In addition, based on partial power conversion technologies, partial power two-port and three-port topologies are analyzed in detail. Their efficiency and power density can be further improved by the combination of three-port and partial power conversion technologies. Moreover, comparisons among seven different types of distributed PV systems are presented with their advantages and disadvantages. Compared to distributed PV systems without energy storage, distributed PV systems with hybridization of energy storage and with partial power regulation can use solar energy in a more efficient way.

Keywords: battery storage system; distributed PV system; partial power regulation; three-port converter

1. Introduction

Photovoltaic (PV) systems are well known for their potential in green energy with the advantages of pollution-free power generation and low-cost operation and maintenance [1,2]. The main problem with PV systems is the uncertainty of the generated power, which depends on the weather [3,4]. To avoid energy waste and fulfil output requirements, energy storage-integrated PV power systems are used, normally with two individual DC-DC power converters [5–7]. One of the converters delivers the PV power to the load and/or battery with the implementation of maximum power point tracking (MPPT) algorithms. The other converter functions as a load power regulator. All the power generated by PV modules and/or battery is processed through these DC-DC converters, leading to limited efficiency of the whole PV system, low power density, and high costs [8,9].

Up to now, a variety of three-port converters (TPCs)—with a renewable energy input port, an energy storage input/output port, and a load port—have been proposed to improve power conversion efficiency and the power density of the overall circuit [10,11]. They can be categorized into three types: fully isolated, partly isolated, and non-isolated TPCs [12–14]. With the advantages of galvanic isolation between the ports and high voltage gain, fully isolated TPCs are commonly equipped with multi-winding transformers and groups of active power switches [15]. However, using transformers and multiple switches increases both the system's volume and cost. In applications where not all ports need isolation, partly isolated TPCs are an option, allowing for higher power density and reduced volume [16]. In cases where galvanic isolation is unnecessary, non-isolated TPCs

are preferred, offering benefits such as greater efficiency, higher power density, smaller size, lower costs, and simpler control compared to the other types of TPCs [17]. In addition, some TPCs with partial power regulation (PPR) have been proposed to further improve the power conversion efficiency of the whole PV power system [18,19].

Moreover, PV panels are usually connected in series to cope with high voltage and power requirements [20]. For these internal connections of PV panels, partial shading situations are frequently encountered, causing some issues such as the diminution of the output voltage and power, some hot spots in the panels, and reduction of the system lifetime [21]. To overcome these problems, the distributed PV system with distributed maximum power point tracking (DMPPT) was introduced [22,23]. In this system, each solar panel is connected to an individual DC-DC converter to supply the energy to the load. With such a configuration, every PV panel can be operated at the maximum power point (MPP) by regulating its associated converter, avoiding energy waste. However, since the energy generated by the PV panel highly depends on the weather conditions, the PV power varies with the time. Mismatches between the generated PV power and the required load power may happen. When the power generated by the PV panels is higher than the load power, to maintain the generated and delivered power at the same level, either a PV power curtailment algorithm [24] is needed to reduce the generated PV power to the load power level, or a BESS is required to be connected to the PV systems to absorb the surplus PV power. Compared to the employment of a PV power curtailment algorithm, the PV power in BESS-integrated PV systems is optimally used, avoiding energy waste [25].

This work explores three-port and partial power conversion technologies for PV generators. The main contributions include a detailed discussion and comparison of various TPCs, focusing on power conversion efficiency and component characteristics. It also analyzes TPCs with partial power regulation through prototype examples, highlighting their advantages and disadvantages. Additionally, the benefits and drawbacks of distributed PV systems with and without a BESS are examined in detail. This study aims to provide foundational knowledge in the field of three-port and partial power conversion, serving as a reference and groundwork for future developments.

The paper is organized as follows. Section 2 presents PV power systems. Section 3 describes three-port electrical converter technologies. Section 4 presents three-port converters with partial power regulation. Section 5 presents PV systems with distributed architecture. Finally, Section 6 summarizes the conclusions.

2. PV Power Systems

In general, PV power conversion systems can be categorized into three types: stand-alone, hybrid, and grid-connected power systems, depending on the load types [26].

2.1. Stand-Alone PV Systems

The stand-alone systems are usually located on a remote area without a connection to the utility mains [27]. Because the power generated by PV panels is unstable and unpredictable, an imbalance between the generated and the delivered power may occur. This imbalance may cause power fluctuations that can damage the equipment connected to the PV system. Thus, to solve imbalance issues, energy storage is commonly integrated into the system as a back-up power supply that can complement the PV power [28]. When the generated PV power is higher than the required load power, the energy storage absorbs the excess energy, whereas the stored energy in the energy storage is delivered to the load to complement the lack of power when the power generated by the PV panels is lower than the load power requirements. The energy storage in PV systems could be a BESS, supercapacitors, flywheels, pumped hydro, superconductors, or compressed air [29].

Figure 1 shows the configuration of a stand-alone PV power conversion system. The generated PV power is transmitted to the load through a DC-DC converter with the implementation of an MPPT algorithm. Also, the BESS is equipped with a DC-DC converter

to supply the energy to the load or absorb the surplus power generated by the PV panels. The load could be DC loads or/and AC loads through a DC-AC inverter.
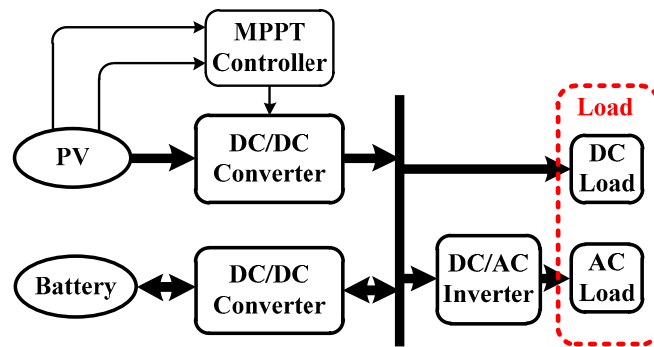

Figure 1. Stand-alone PV power conversion system.

2.2. Hybrid PV Systems

Generally, hybrid PV systems are composed of several different types of power sources, such as diesel fuel generators, with the integration of energy storage [30]. Due to the employment of auxiliary generators, the systems have high supply reliability as the utility mains, but the costs increase.

Figure 2 depicts the configuration of a hybrid PV power conversion system, consisting of PV panels, a BESS, two DC-DC converters, a DC-AC inverter and auxiliary generators. Under a high solar radiation level situation, the total load power is supplied by the PV panels and the surplus generated PV power is stored in the BESS. When there is a situation of insufficient sunlight and the energy storage can no longer supply the load power requirements, the generators provide the energy to the load and charge the battery.
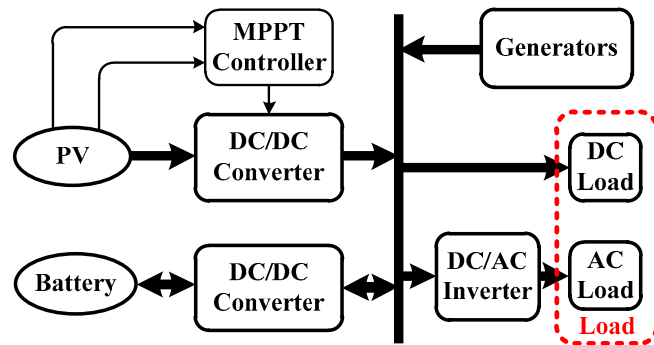

Figure 2. Hybrid PV power conversion system.

2.3. Grid-Connected PV Systems

The output of grid-connected PV systems is connected to the AC grid through a DC-AC inverter, as shown in Figure 3. The system can be subdivided into two types: central and decentralized grid-connected PV systems [31]. Compared to the decentralized grid-connected PV systems, the central grid-connected PV systems have a wide power range that can feed directly into medium- and high-voltage grids [32,33].

For power systems with a high share of PV generation, frequency fluctuation is a frequently encountered issue, which can negatively impact the power system, because PV power is highly affected by weather conditions and the incidence angle of light and shading [34]. Introducing power curtailment and providing energy storage systems are the most common solutions for frequency stability problems [35].
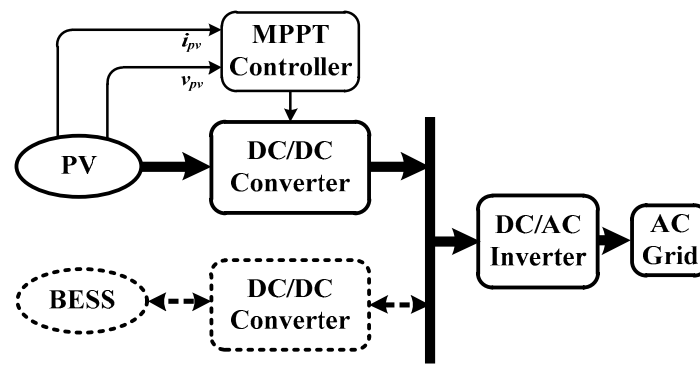
Figure 3. Grid-connected PV power conversion system.

- *PV power curtailment methods*

Figure 4 illustrates an alternative grid-connected PV system with a power curtailment control algorithm. The advantages of this method are a more straightforward implementation and a lower initial investment. When the PV power curtailment method is implemented, the power generated by the PV panels is lower than the maximum PV power, meaning that the operating point is at a suboptimal power level [36]. Therefore, the current–voltage (I-V) curve and the actual MPP need to be estimated to determine the available power. There are several existing and proposed methods for estimating the maximum available power point while operating suboptimally, which can be categorized into two types: measurement-based and curve-fitting-based methods [37,38].
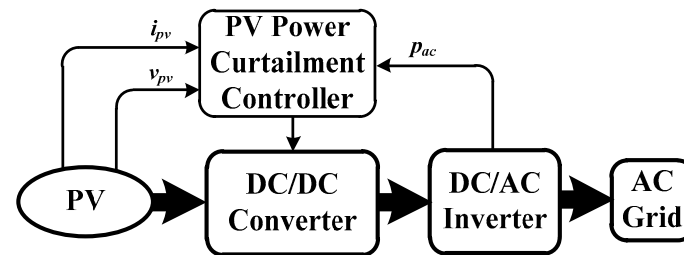

Figure 4. Alternative grid-connected PV system control with power curtailment control algorithm.

In measurement-based methods, additional sensors, such as temperature and irradiance sensors, are required for measuring the real-time operating point [39]. With these additional sensors, the measurements are more accurate. Thus, the implementation of the control strategy is effective. However, due to the employment of additional sensors in the PV system, its cost and complexity may increase.

For curve-fitting-based methods, curve fitting with a number of PV voltage and current samples is used for the estimation of the entire I-V curve. The Newton quadratic interpolation (NQI) or nonlinear least squares is commonly used to solve curve-fitting problems. The accuracy of NQI, influenced by the selection of three sample points, has been discussed in [40]. The results of the nonlinear least-squares curve-fitting technique are highly affected by the initial values and noise, which have been analyzed in detail in [41].

In reference [40], two current–voltage points were used to estimate the open-circuit current, allowing the MPP to be calculated using an empirical expression for power curtailment. While this method is simpler to implement, it is highly sensitive to noise.

In work [41], nonlinear least-squares curve-fitting was used to estimate the actual I-V curve, the power–voltage (P-V) characteristic, and the MPP. The operating point can be operated on both sides of the P-V curve. A control strategy based on the PV voltage was proposed to regulate pulse-width modulation (PWM) for adjusting the output power of the boost converter to fulfil the grid power requirements. Additionally, an effective approach

was proposed to address instability issues arising from sudden changes in irradiance and temperature.

In [42], the P-V characteristic and the MPP were estimated by curve fitting. A PV power curtailment method with the ripple control algorithm was proposed for the adjustment of a two-stage inverter. The system is operated on the right side of the MPP, resulting in instability of the system when step changes occur in the irradiance, but higher efficiency is achieved.

In reference [43], one PV string within the array operated as an auxiliary string to implement the MPPT algorithm and determine the available power. The remaining PV strings worked together to maintain constant power generation, meeting the AC power demand. However, this method faces challenges: variations in shading levels across strings can lead to inconsistencies, and the communication required among strings may increase operational complexity.

In [44], the desired power was determined through offline calculations based on PV module datasheet values. This method enables a fast frequency response and high accuracy, though it requires additional sensors to precisely measure temperature and irradiance.

In reference [45], a method based on the estimation of the power losses of electronic power converters that connect the PV panel to the AC grid was proposed, avoiding mismatches between the generated and delivered power.

Table 1 summarizes the main characteristics of the mentioned PV power curtailment methods.

Table 1. Different types of photovoltaic power curtailment methods.

Method	Estimation Output	Operation Side	Controlled Variable	PV Configuration	Converter Losses
[40]	MPP	Left	Duty cycle	Single-stage	Neglected
[41]	MPP and P-V curve	Left or right	PV voltage	Single-stage	Neglected
[42]	MPP and P-V curve	Right	PV power	Double-stage	Neglected
[43]	MPP	Left	PV voltage	Double-stage	Neglected
[44]	MPP	Right	PV voltage	Single-stage	Neglected
[45]	MPP and P-V curve	Left	PV voltage	Double-stage	Considered

- *Integration of energy storage*

Another approach to reduce the power system's frequency fluctuations is the integration of energy storage with grid-connected PV systems [46–48], as shown in Figure 3 (with the dashed lines). The power fluctuations, which may be short-term ranging from seconds to hours, caused by the PV power variation, are absorbed by the energy storage. Thus, the power fluctuations are not transferred to the AC grid, increasing the stability and reliability of the power system, especially in the case of power systems that do not have a sufficient spinning reserve [49].

Moreover, in the case of low-voltage conditions in the grid, large-scale PV systems are required to remain connected to the power system, but the amount of power that can be injected into the grid is limited. This causes energy accumulation in PV systems, increasing the voltage in intermediate stages, and instabilities and stress on the power converter system. This instability makes it difficult for PV systems to remain connected during the recovery period. In this case, the energy storage can significantly contribute to keeping the system stable with the capability to absorb energy during low-voltage periods as well as to avoid energy waste [27].

Compared to the PV power curtailment method, the power fluctuation pressure on grids with energy storage-integrated grid-connected PV systems is lower and the PV power is used in a more efficient way [50,51].

In recent years, many energy storage technologies, such as superconducting magnets, pumped hydro, ultracapacitors, and BESSs, with their control methods, have been proposed to smooth PV power output [52,53]. For superconducting magnetic storage systems

and ultracapacitors, the energy densities are low, and therefore, they are usually used in pulsed-power and system-stability applications. For pumped hydro, it has topographical limitations, and therefore, it is not suitable for large-scale PV systems in flat areas [26]. Since BESSs have the advantages of high power density, long cycle life, and a fast response time, they are widely used in PV systems as energy storage [27].

Also, numerous control methods for reducing power fluctuations generated by energy storage-integrated PV systems have been proposed, for example, in [54,55].

In reference [56], a ramp rate control based on the moving average of an electric double-layer capacitor was proposed. The PV output can be changed at a limited ramp rate, because the rapid fluctuations generated by the PV panels are absorbed by the capacitor. The capacitor is maintained at a specified voltage, so there is no need for a high capacitance.

Reference [57] presents a control strategy with the control of the PV output ramp rate. To mitigate the power fluctuation, the energy storage is deployed by using PV output ramp rate to control the PV inverter ramp rate to a desired level.

3. Three-Port Electrical Converter Technologies

3.1. Traditional Configuration of BESS-Integrated PV Systems

Conventionally, a BESS-integrated PV system consists of two individual two-port power electronic converters [58]. One of them is interposed between the PV module and the load, which is unidirectional, delivering the PV power to the load and/or battery with the implementation of MPPT. The other DC-DC converter, which is bidirectional, is connected to the BESS, and functions as a load power regulator.

The configuration of a traditional PV system with a BESS is shown in Figure 5. With the employment of an additional two-port DC-DC converter connected to the BESS, more components and power conversion stages are used, leading to limited efficiency, low power density, and high costs.
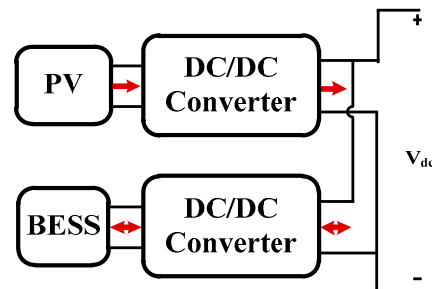

Figure 5. Traditional configuration of a PV system with two individual DC-DC converters. The red lines indicate the possible directions of power flow.

3.2. Three-Port Converters

Some circuits with TPC technology instead of two individual DC-DC converters have been proposed to overcome the low efficiency, low power density, and high cost issues of traditional PV systems [59,60]. DC-DC converters equipped with a PV panel and a BESS were integrated into a TPC, resulting in only one power conversion stage between any two ports. Figure 6 illustrates the power flow scheme of traditional TPCs, which include three ports: a PV input port, an energy storage port, and a load port. The PV input port is a unidirectional port that could be a string or array of PV modules. The energy storage port is a bidirectional port that could be connected to supercapacitors and BESSs, which can supply energy to the load and receive power from the PV source. The load port is unidirectional and could be connected to DC loads, such as LEDs and DC motors, or AC loads or an AC grid, through a DC-AC inverter.
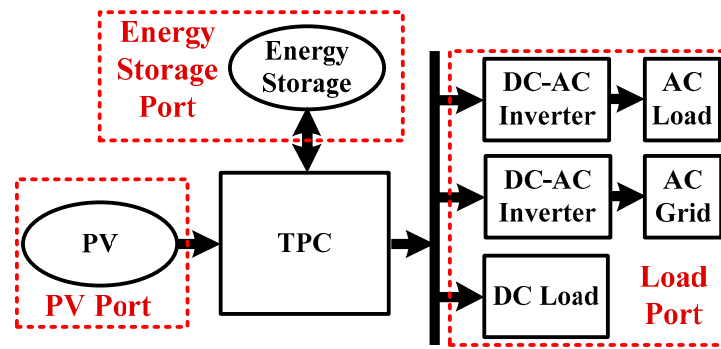
Figure 6. Power flow scheme of traditional TPCs.

Generally, the power flows among the three ports of a TPC depend on the relationships among the PV power, the BESS power, and the load power [61]. Figure 7 illustrates the operational modes of a TPC (the arrows indicate the power flows), which can be divided into three modes: single-input dual-output (SIDO), dual-input single-output (DISO), and single-input single-output (SISO) modes. When the generated PV power is higher than the load power, the load receives energy from the PV panel through the TPC and the excess PV power supplies the BESS. Thus, the BESS port performs as an output port, and the system enters SIDO mode (Figure 7a). When the PV power is lower than the load power, the TPC is operated in the DISO mode (Figure 7b), as two input DC sources, the BESS and PV, supply energy to the load. For the SISO mode (Figure 7c–e), only one input source and one output port are turned on. This means that one of these three ports (PV port, load port, and BESS port) in the PV system consumes zero power or does not generate any power.
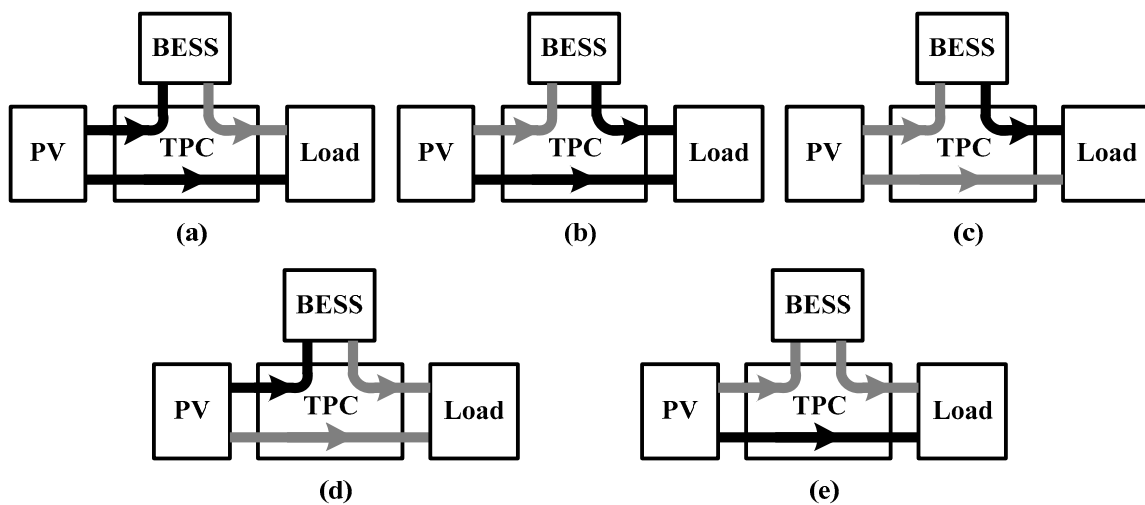

Figure 7. Power flow scheme of traditional TPCs. Operation modes of a TPC: (**a**) SIDO; (**b**) DISO; (**c**–**e**) SISO.

TPCs can be categorized into three types: fully isolated, partly isolated, and non-isolated.

- *Fully isolated TPCs*

Traditional full-bridge converters and half-bridge converters are commonly used to construct fully isolated TPCs. Since multi-winding transformers and a group of active power switches in full- and half-bridge converters are used, high voltage gain and galvanic isolation between ports can be achieved. But this type of topology has the disadvantages of higher complexity, higher costs, and a larger size [62–65] than partly isolated and non-isolated TPCs. Table 2 presents a comparison of fully isolated TPCs.

Table 2. Comparison of fully isolated TPCs.

Topologies	Diodes	Inductors	Switches	Capacitors	Rated Power (W)	Efficiencies (%)
[62]	0	1	12	1	1000	88–96
[63]	0	3	6	6	2500	90–92
[64]	1	2	12	3	220	78–91
[65]	0	1	6	7	6000	86–91

In reference [62], an optimal idling control strategy for multi-port converters (MPCs) was proposed. The advantages of MPCs are their simple system structure and low cost. Moreover, MPCs provide an idling port with zero power if one of the ports is disconnected from the system. To ensure low conduction losses, a control strategy based on phase-shift and PWM controls is proposed with a wide soft-switching operation range.

In work [63], an asymmetrical duty cycle control method for a fully isolated TPC with three half-bridge converters is proposed. A wide zero-voltage-switching (ZVS) range for each port under variable ultracapacitor and battery voltages can be achieved with a constant DC bus voltage regulated by asymmetrical duty cycle and phase shift control.

Reference [64] presents a system architecture with two modules of a three-port isolated DC-DC converter connected in parallel. A control method with an adapted power sharing algorithm was used to improve the global efficiency of the system.

In reference [65], an energy storage-integrated DC-DC converter with a combination of high power density and multiple inputs was proposed. Soft switching can be achieved without auxiliary devices and components. With the equipment of a half-bridge to each port, the power flow between the input and output is achieved by the regulation of the phase shift angles of the voltages across the two sides of the transformer.

- *Partly isolated TPCs*

As only two ports in TPCs need to be isolated, partly isolated TPCs can be used [66–69]. Partly isolated TPCs can fulfil the galvanic isolated requirements between two of the three ports. Compared to isolated TPCs, generally fewer components are utilized, resulting in high power density and small volume. Since the voltage difference between the PV port and the energy storage port is usually small, circuit topology with isolation between the PV and energy storage ports and the load port is widely used. Table 3 presents a comparison of partly isolated TPCs.

Table 3. Comparison of partly isolated TPCs.

Topologies	Diodes	Inductors	Switches	Capacitors	Rated Power (W)	Efficiencies (%)
[67]	2	3	6	3	800	89–94
[66]	4	3	4	3	400	90–93
[68]	3	2	4	3	250	87–91.3
[69]	4	3	3	5	500	50–96

Reference [67] presented a proposal of a full-bridge TPC with PWM plus secondary phase shift. A control strategy with two control degrees of freedom is used to regulate the voltage and the power and to achieve ZVS of both the primary and secondary side switches.

In reference [66], a full bridge TPC with the integration of two buck-boost converters into the primary side of the full-bridge topology was proposed. The advantages of this topology are that the power conversion between any two of the three ports is single-stage, and ZVS of all the primary side switches are achieved, resulting in high power density and efficiency.

In [68], based on an improved flyback-forward circuit, a partly isolated circuit was proposed with a decoupled port control for stand-alone PV systems. The advantages of this topology are high power capability, system simplicity, and low cost.

Reference [69] presented a partly isolated topology with an input boost converter for PV–battery power supply applications. By adding an input boost converter based on magnetic switching, the PV current is continuous, and the input voltage is stepped up. Additionally, zero current switching (ZCS) technology is used to achieve high power conversion efficiency.

- *Non-isolated TPCs*

In non-isolated TPCs, galvanic isolation is not critically required [70–75]. The topology is mostly based on buck, boost, and buck–boost converters, resulting in limitations of the voltage gain. To achieve high voltage gain, some non-isolated TPCs with coupled inductors are proposed. Compared to fully and partly isolated TPCs, non-isolated TPCs use fewer components, resulting in higher efficiency, higher power density, smaller size, lower cost, and simpler control.

In reference [18], a TPC for energy storage-integrated PV systems was proposed with only one inductor and two power switches. Due to the employment of partial power regulation, the power conversion efficiency is improved.

Reference [70] presented a high voltage gain topology with the advantages of continuous input current with a low ripple and low voltage stress on the switches, resulting in high efficiency.

In reference [71], a non-isolated TPC was proposed without the use of multiple windings that reduce the costs and the volume. A power control strategy was proposed based on large- and small-signal models.

In reference [72], a fully reconfigurable topology with a single inductor was proposed. Since it uses just one inductor, the density is improved, and the volume is reduced. In addition, single-stage power conversion between any two of three ports can be achieved.

In [73], the topology has the advantages of high voltage gain without the employment of a transformer and low voltage stresses on switches. In [72], a higher voltage gain was achieved without the use of coupled inductors and voltage multiplier cells.

Nevertheless, in [70–74], a number of components (including switches, capacitors, transformers, and inductors) were used, resulting in higher control complexity, lower efficiency, and higher costs. In [75], a soft-switching TPC was proposed with ZVS and leakage inductor energy recycling. However, the complexity of the control increases with the number of power switches and an active clamp circuit.

A summary of the characteristics of the mentioned non-isolated TPCs is shown in Table 4.

Table 4. Comparison of non-isolated TPCs.

Topologies	Diodes	Inductors	Switches	Capacitors	Rated Power (W)	Efficiencies (%)
[18]	0	1	2	3	15	95.4–99.68
[70]	5	2	3	4	100	91–94
[71]	2	2	2	2	100	85–94
[72]	5	1	4	3	50	87.8–93
[73]	1	2	4	4	1000	96–98
[74]	5	2	3	4	200	86–99
[75]	2	1	5	3	300	94.2–96.8

4. Three-Port Converters with Partial Power Regulation

4.1. Two-Port Partial Power Converters

Traditionally, a full power electronic converter (FPC) is connected to the PV module to meet the load requirements and to implement the MPPT algorithm [76]. The circuit configuration and power flow scheme are shown in Figure 8a and 8b, respectively. In a PV system employing an FPC, all PV power is transferred to the load through a DC-DC converter, reducing the power conversion efficiency. To improve the efficiency of the whole PV system, partial power converters (PPCs) are proposed. Only a fraction of the PV power is processed by the DC-DC converter to the load, which can significantly reduce the power

losses and the volume [77,78]. Figure 9a and 9b show the circuit configuration and power flow scheme of PPCs, respectively. As can be seen in these figures, an additional direct power flow path from the PV to the load (red lines) is used. Since the losses on the direct power path are negligible, the efficiency is improved, and the voltage and current pressures on the key components, such as inductors, switches, and diodes, are reduced [79].
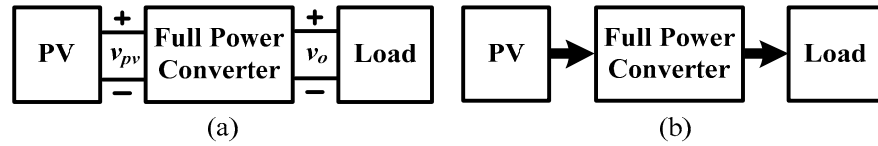

Figure 8. Full power converter. (**a**) Circuit configuration. (**b**) Power flow scheme.
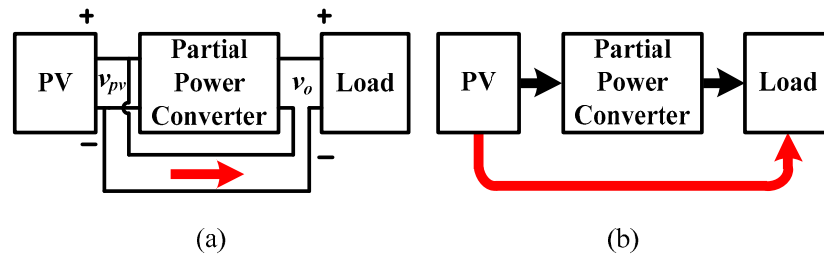

Figure 9. Partial power converter. (**a**) Circuit configuration. (**b**) Power flow scheme (red arrows indicate direct power flow).

The basic idea of PPCs is that a connection between the PV panel and the load, as shown in Figure 10a (red arrow), is added to a FPC to reduce the power rating. As can be seen in Figure 10a, part of the PV power is transferred to the load through this path (red arrow) with almost 100% efficiency. Another part is processed through a full power converter, with efficiency η_c, to the capacitor C (blue arrow) or returned to the capacitor C_{pv} connected to the PV panel (green arrow), depending on the circuit operation modes. When v_c is positive, the circuit is operated in the step-up mode, whereas the step-down mode is entered if v_c is negative. Figure 10b and 10c show two examples of step-up operation with buck–boost and flyback converters, respectively. Figure 10d and 10e illustrate two examples of step-down operation with boost and flyback converters, respectively. Points (a), (b), (c), and (d) in Figure 10b–e relate to the points in Figure 10a.

In fact, PPCs are special connections of full power converters [80–82]. A variety of PPCs based on FPCs, such as CUK converters [83], SEPIC converters [84], and synchronous-rectification LLC resonant converters [85], have been proposed. Figure 11 shows the difference between full power boost converters and boost type PPCs as an example. Compared to full power boost converters (blue dashed line) with a power rating of 1, partial power boost converters have a reduced power rating range from 0 to 1, due to the special connection between the PV panel and the load (red dashed line) with almost 100% efficiency. The power rating in the partial power boost converter depends on the voltage ratio between v_{pv} and v_L [86]. Table 5 presents a comparison of PPCs.

Table 5. Comparison of PPCs.

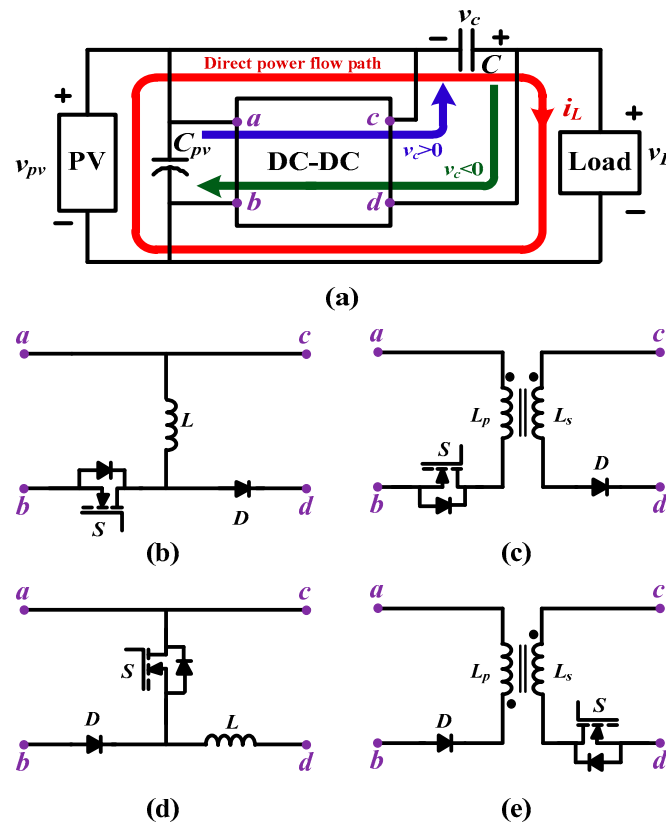| Topologies	Diodes	Inductors	Switches	Capacitors	Rated Power (W)	Efficiencies (%)
[79]	4	2	5	3	822	90–99
[81]	6	1	1	2	45	93.8–95.5
[82]	0	2	12	5	3500	97.9–99.3
[83]	1	2	1	2	200	-
[84]	4	3	2	4	100	94–97
[85]	2	2	8	4	100	93–96.74

Figure 10. Power flow of two-port partial power converters (**a**) with step-up ($v_c > 0$) or step-down ($v_c < 0$) operation modes. (**b**,**c**) Two examples of circuit structure of step-up operation. (**d**,**e**) Two examples of circuit structure of step-down operation.
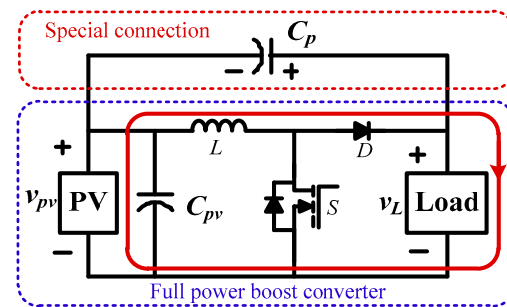

Figure 11. Partial power boost DC-DC converter.

4.2. Three-Port Converters with Partial Power Regulation

The concept of partial power regulation in two-port converters has been introduced in TPCs. Therefore, different circuit topologies combining PPR and TPC techniques have been proposed [18,19].

Figure 12a–c show the power flow scheme of full power TPC, step-down TPC with PPR, and step-up TPC with PPR, respectively. Compared to full-power TPCs (Figure 12a), two additional power flow paths are employed in TPCs with PPR (Figure 12b,c), resulting in high power conversion efficiency and lower voltage and current pressures on the key components.
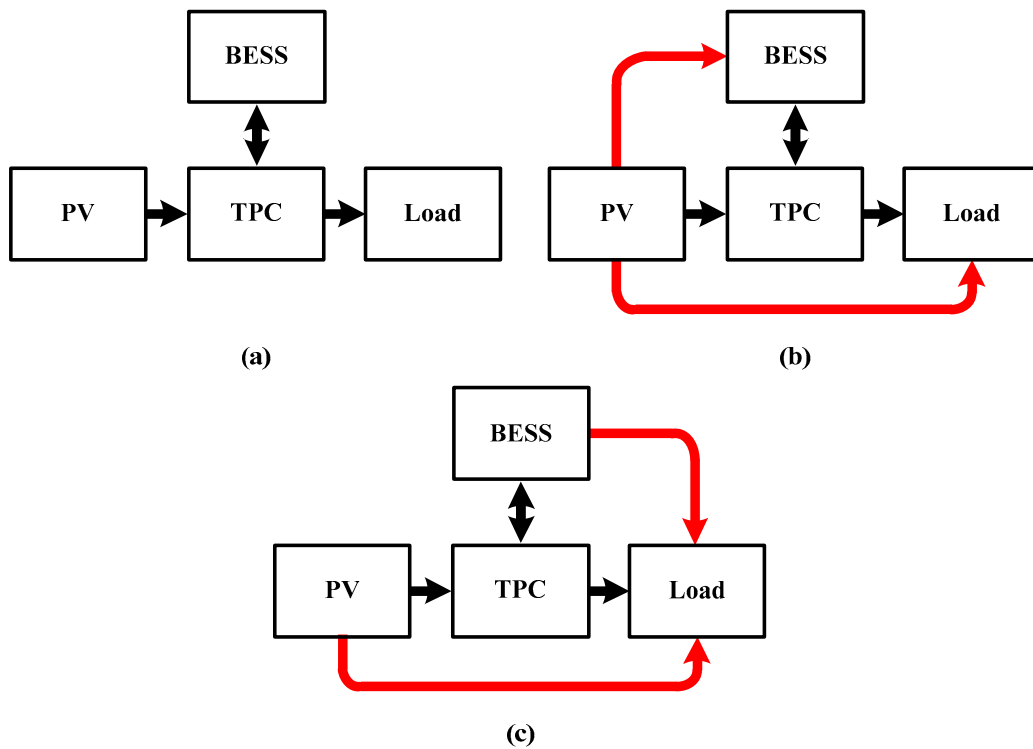
Figure 12. Power flow scheme. (**a**) Full-power TPC; (**b**) step-down TPC with PPR; (**c**) step-up TPC with PPR.

Figure 13 illustrates the power flow scheme of a BESS-integrated PV system connected to a DC-DC converter or a DC-AC inverter with PPR. As can be seen in this figure, the PV panel, the BESS, and the output of the PV system are connected in a series; thus, a direct power flow path (red line) is created to reduce the power rating. The power between any two of the three ports (the PV panel, the BESS, and the output) is processed through a DC-DC converter, which means that just one stage conversion is employed. When the BESS voltage is positive ($v_b > 0$), the circuit is operated under the step-down mode [18], while if $v_b < 0$, the circuit is operated under the step-up mode [19].
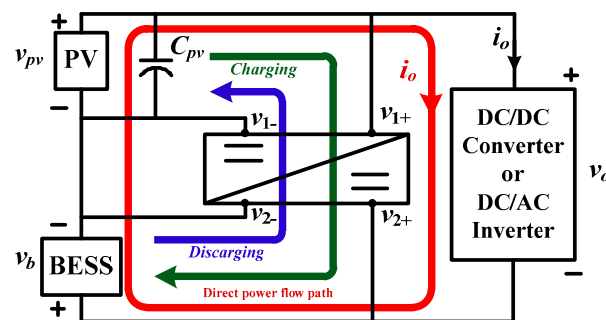

Figure 13. Power flow scheme of the proposed BESS-integrated PV system with PPR.

5. PV Systems with Distributed Architecture

PV panels are generally series—and/or parallel-connected to a power electronic converter to provide high voltage and power. Based on the interconnection of PV systems and the way MPPT is implemented, PV systems can be categorized into two types: centralized and distributed PV systems [87,88].

5.1. Centralized PV Systems

Figure 14 shows a centralized PV power system with a string PV panel. Several PV panels are first connected in series, and then connected to a DC-DC converter or a DC-AC inverter to supply energy to the output. With these inter-connected panels, the output PV current of each PV panel i_{pv} is the same. When partial shading is encountered, not every panel can output its maximum power, which can cause some issues, such as diminution of the output voltage and power, some hot spots in the panels, and reduction of the system lifetime [89].
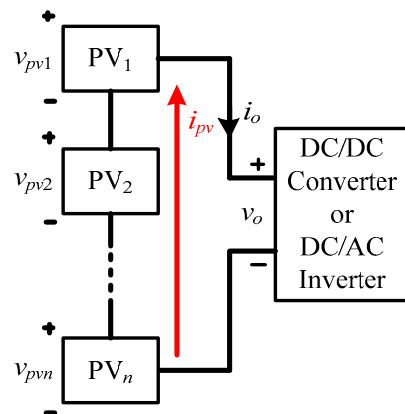

Figure 14. Centralized PV system with a string PV panel.

One approach to overcome these problems is the employment of bypass diodes; another approach is the introduction of distributed PV system architectures with individual converters [90].

For the employment of additional bypass diodes, connected in parallel to the PV panels, paralleled bypass diodes provide an additional current path for the unshaded PV panels, operating at the MPP, as shown in Figure 15. However, the shaded PV panels do not supply any energy to the output when the bypass diodes are turned on to conduct the PV current, resulting in diminution of the PV power [91].
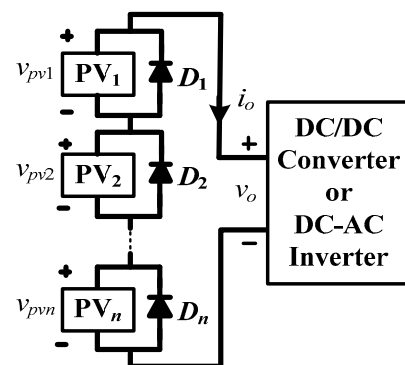

Figure 15. Centralized PV system with bypass diodes.

5.2. Distributed PV Systems

For the latter approach, each solar panel is connected to its associated individual DC-DC converter to supply energy to the output [92]. Each individual converter can achieve MPPT on the associated PV panel. Thus, each PV panel can output its maximum power. Figure 16 shows a traditional distributed PV system with individual converters. As can be seen in this figure, the output voltage, v_o, and power, p_o, are limited if each solar panel is operated at the MPP, because the generated PV power highly depends on the weather conditions, and the output currents (i_{o1}, i_{o2} ... i_{on}) of each converter are identical. When the required output power is lower than the overall PV power, an additional power

curtailment algorithm is required, which increases the complexity of the control and reduces the reliability of the PV system. In addition, the use of full-power DC-DC converters in this PV system architecture results in low power conversion efficiency.
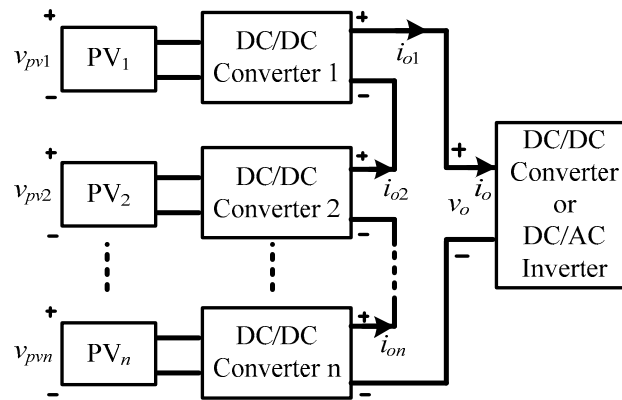

Figure 16. Traditional distributed PV system with individual converters.

To improve the efficiency, some architectures with PPR have been proposed [93,94], as shown in Figures 17–19. As can be seen in these figures, the PV panels are connected in series with the output so that they can supply a part of the PV power to the output directly, resulting in high efficiency.
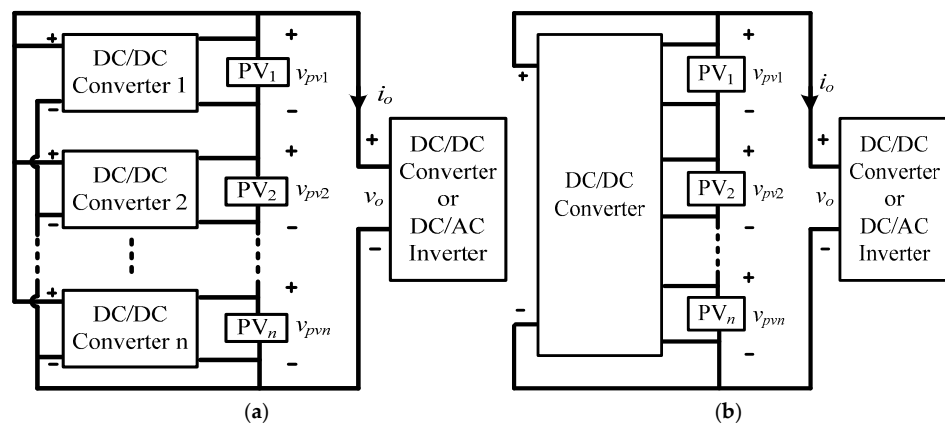

Figure 17. Distributed PV system architectures. (**a**) Individual DC-DC converters connected between each PV panel and the output. (**b**) A DC-DC converter connected between PV panels and the output.
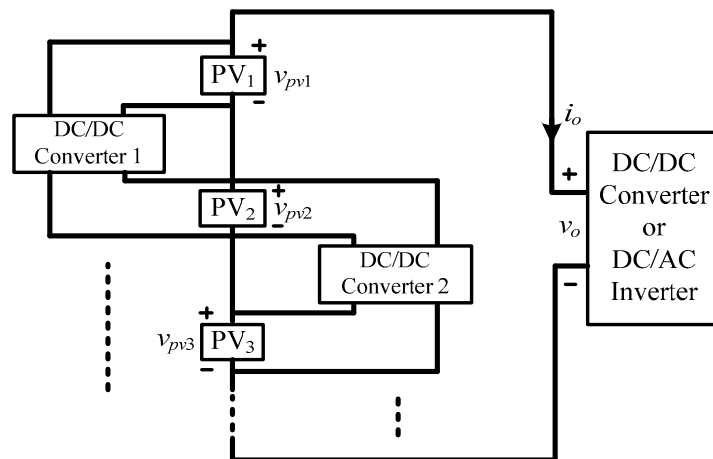

Figure 18. Distributed PV system architecture with DC-DC converters connected between each PV panel.
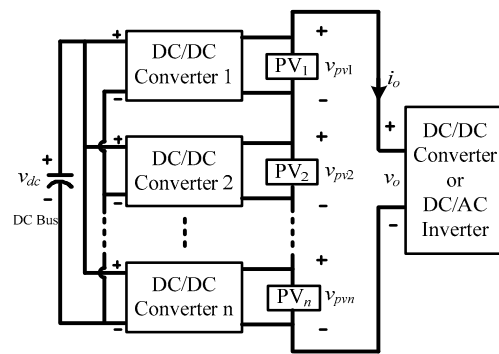
Figure 19. Distributed PV system architecture with DC-DC converters connected between each PV panel and the DC bus.

Figure 17a and 17b show distributed PV system architectures with each DC-DC converter connected between a PV panel and the output and with a DC-DC converter connected between the PV panels and the output, respectively. As can be seen in these figures, each PV panel can output its maximum power at multiple string current levels. However, in Figure 17a, due to the direct connection of the negative of input and output, isolated DC-DC converters are required [95]. In Figure 17b, the DC-DC converter is a multi-port converter, which could be different types of converters, such as a multi-winding converter [96] or a switched-capacitor converter [97].

A switched-capacitor converter was proposed in [97] for PV systems with differential power processing. Instead of inductors, ceramic capacitors are employed, resulting in lower costs and smaller volume. However, the main disadvantage of this architecture is the flexibility of the conversion ratio in most cases, reducing the reliability of the PV system when the weather conditions frequently change.

An architecture based on battery equalizer was proposed in [98], with the advantage of just using one inductive storage element. However, only one inductor to process the PV power to the output results in high current pressure on the inductor.

Additionally, since the output voltage, v_o, is the sum of the PV voltages on n solar panels (v_{pv1}, $v_{pv2} \ldots v_{pvn}$), the voltage difference between the output and each PV panel is high if a long-string PV module is used. Therefore, a high voltage step-up ratio of each DC-DC converter is needed, increasing the pressures on the converters.

Figure 18 shows a distributed PV system architecture with a DC-DC converter connected between each PV panel. The main advantage of this architecture is that the voltage ratios of DC-DC converters are not affected by the load voltage, reducing the voltage rating [99]. However, when the PV string length increases, the maximum power processed by any DC-DC converter increases [100]. This causes an increase in the required current rating with the PV string length. Moreover, the distributed MPPT algorithm is required for easy scalability.

Figure 19 shows a distributed PV system architecture with DC-DC converters connected between each PV panel and a DC bus. Compared to the architecture in Figure 17, the outputs of DC-DC converters are connected to a DC bus, which is independent from the load. This means that a high voltage ratio is not critically required, reducing the costs. However, bidirectional DC-DC converters are needed to draw the power into and out of the independent DC bus to maintain the DC bus voltage [101,102]. Since the power balance on the DC bus has to be kept, an accurate MPPT may not be achieved at any given PV string current [103].

For the system architectures in Figures 16–19, the load power varies when the weather conditions change. When the power generated by the PV panels is higher than the load power, a PV power curtailment algorithm is implemented, or a BESS is integrated into the PV systems. By introducing the BESS, when the power generated by the PV panels exceeds the required load power, the surplus PV power can be absorbed by the BESS. When the

generated PV power is lower than the required load power, the BESS can supply energy to the load to keep the load voltage and power constant, avoiding energy waste.

Distributed PV systems with a hybridization of a BESS and PPR were proposed in [18,19]. Figure 20 shows the circuit configuration of the distributed PV system with a BESS and PPR. Each PV panel with an individual DC-DC converter is connected to a BESS in series as a PV-BESS module to supply energy to the load. Since PV panels and BESSs are connected in series, part of the PV power is supplied to the output and BESSs directly, improving efficiency. Moreover, due to the employment of a BESS and an independent DC-DC converter in each module, the implementation of the MPPT algorithm is not affected by the output requirements or the input PV power. This means that each PV panel can supply its maximum power even if the required output power is lower than the generated PV power, utilizing the PV power in an efficient way. A step-up distributed PV system architecture with its detailed circuit analysis was proposed in [19] for the DMPPT. A step-down topology for distributed PV systems was also proposed in [18], which can reduce the voltage pressure on the output when a long string of PV-BESS modules is used.
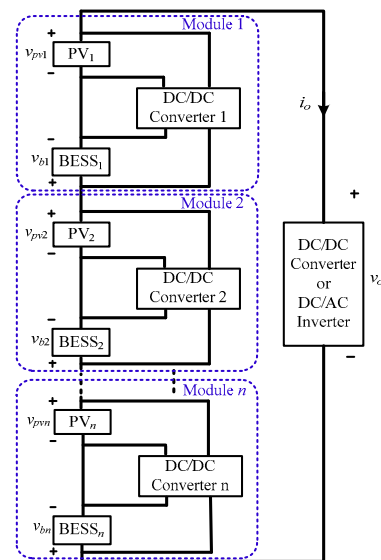

Figure 20. Circuit configuration of a distributed PV system with a BESS and PPR.

6. Conclusions

In this paper, the advantages and disadvantages of three-port and partial power conversion technologies have been analyzed in detail to help in the selection and design of PV systems. A comparison of TPCs and distributed PV systems has been presented. Compared to PV systems with two-port converters, PV systems with TPCs have the advantages of higher efficiency and power density. Based on the need for galvanic isolation, TPCs can be classified into three types: fully isolated, partly isolated, and non-isolated. Fully isolated TPCs typically achieve high voltage gain but come with a larger volume and higher cost. Partly isolated TPCs provide partial isolation between two of the three ports, offering higher efficiency and power density. Compared to the other two types, non-isolated TPCs have the advantages of higher efficiency, greater power density, a smaller size, and lower cost.

In addition, compared to FPCs, PPCs reduce power losses and volume. By employing partial power technology in TPCs, the efficiency and power density can be further improved. Moreover, solar energy can be used in an efficient way by employing TPCs and partial power regulation in distributed PV systems with energy storage. This setup also simplifies the implementation of the DMPPT, as each PV panel is equipped with its own energy storage.

This article can be used as a guide for selecting TPCs and distributed PV system architectures for different applications.

References

1. Tian, Q.; Zhou, G.; Leng, M.; Xu, G.; Fan, X. A Nonisolated Symmetric Bipolar Output Four-Port Converter Interfacing PV-Battery System. *IEEE Trans. Power Electron.* **2020**, *35*, 11731–11744. [CrossRef]
2. Belloni, E.; Massaccesi, A.; Moscatiello, C.; Martirano, L. Stand-Alone LED Lighting System Powered by PV and Battery: Electrical Overall Performance Analysis of a Case Study. *IEEE Trans. Industry Appl.* **2024**, *60*, 5142–5149. [CrossRef]
3. Touré, M.L.; Camara, M.B.; Dakyo, B. Symmetrical Multilevel High Voltage-Gain Boost Converter Control Strategy for Photovoltaic Systems Applications. *Electronics* **2024**, *13*, 2565. [CrossRef]
4. Myneni, H.; Ganjikunta, S.K. Energy Management and Control of Single-Stage Grid-Connected Solar PV and BES System. *IEEE Trans. Sustain. Energy* **2020**, *11*, 1739–1749. [CrossRef]
5. Kurm, S.; Agarwal, V. Dual Active Bridge Based Reduced Stage Multiport DC/AC Converter for PV-Battery Systems. *IEEE Trans. Ind. Appl.* **2022**, *58*, 4027–4035. [CrossRef]
6. Hasabelrasul, H.; Cai, Z.; Sun, L.; Suo, X.; Matraji, I. Two-Stage Converter Standalone PV-Battery System Based on VSG Control. *IEEE Access* **2022**, *10*, 39825–39832. [CrossRef]
7. Chen, Q.; Zhu, B.; Mao, S. Analysis of Grid-Connected Stability of VSG-Controlled PV Plant Integrated with Energy Storage System and Optimization of Control Parameters. *Electronics* **2024**, *13*, 1314. [CrossRef]
8. Tang, X.; Chen, X.; Zhang, R.; Li, Q.; Song, Y.; Zhang, Y.; Luo, N. The Averaged Modeling Method and Power Fluctuation Smoothing Research of the Two-Stage PV and Battery Hybrid System. In Proceedings of the 2020 10th International Conference on Power and Energy Systems (ICPES), Chengdu, China, 25–27 December 2020.
9. Hasan, M.M.; Jaman, S.; Geury, T.; Hegazy, O. Design and Simulation of a Grid-Connected Two-Stage Bidirectional Converter for a Combined PV- Stationary Energy Storage System. In Proceedings of the 2022 Second International Conference on Sustainable Mobility Applications, Renewables and Technology (SMART), Cassino, Italy, 23–25 November 2022.
10. Saadatizadeh, Z.; Heris, P.C.; Mantooth, A. High-Frequency Three-Port DC–DC Converter with Zero-Voltage Switching Operation. *IEEE Trans. Ind. Electron.* **2023**, *71*, 537–548. [CrossRef]
11. Zhang, H.; Li, Z.; Xue, Y.; Chang, X.; Su, J.; Wang, P.; Guo, Q.; Sun, H. A Stochastic Bi-level Optimal Allocation Approach of Intelligent Buildings Considering Energy Storage Sharing Services. *IEEE Trans. Consumer Electron.* **2024**, *70*, 5142–5153. [CrossRef]
12. Duarte, J.L.; Hendrix, M.; Simões, M.G. Three-Port Bidirectional Converter for Hybrid Fuel Cell Systems. *IEEE Trans. Power Electron.* **2007**, *22*, 480–487. [CrossRef]
13. Sarkar, S.; Nayak, S.; Das, A.; Hu, H.; Xing, Y. A Three Port Three-Phase Modular Series Multilevel Converter Integrating MVDC with MVAC Grids. In Proceedings of the IECON 2023- 49th Annual Conference of the IEEE Industrial Electronics Society, Singapore, 16–19 October 2023.
14. Hameed, A.; Moschopoulos, G. Three-phase Single-stage Multiport Bidirectional AC-DC Converter with Reduced Power Conversion Stages. In Proceedings of the 2024 IEEE Applied Power Electronics Conference and Exposition (APEC), Long Beach, CA, USA, 25–29 February 2024.
15. Sofiya, S.; Sathyan, S. Three-Port Isolated Hybrid Converter for Power Supply Systems in EV. In Proceedings of the 2022 IEEE International Conference on Power Electronics, Smart Grid, and Renewable Energy (PESGRE), Trivandrum, India, 2–5 January 2022.
16. Wu, H.; Sun, K.; Zhu, L.; Xing, Y. An Interleaved Half-Bridge Three-Port Converter with Enhanced Power Transfer Capability Using Three-Leg Rectifier for Renewable Energy Applications. *IEEE J. Emerg. Sel. Topics Power Electron.* **2016**, *4*, 606–616. [CrossRef]
17. Huynh, K.K.N.; Liang, T.; Tran, T.A.A.; Chen, K. Three-Port Converter with Leakage Inductance Energy Recycling for High Step-Down Applications. *IEEE J. Emerg. Sel. Topics Power Electron.* **2023**, *11*, 4453–4462. [CrossRef]
18. Ye, D.; Martinez, S. A Three-Port DC-DC Converter with Partial Power Regulation for a Photovoltaic Generator Integrated with Energy Storage. *Electronics* **2024**, *13*, 2304. [CrossRef]
19. Du, Y.; Lu, D.D. Battery-integrated boost converter utilizing distributed MPPT configuration for photovoltaic systems. *Sol. Energy* **2011**, *85*, 1992–2002. [CrossRef]
20. Bell, R.; Pilawa-Podgurski, R.C.N. Decoupled and Distributed Maximum Power Point Tracking of Series-Connected Photovoltaic Submodules Using Differential Power Processing. *IEEE J. Emerg. Sel. Topics Power Electron.* **2015**, *3*, 881–891. [CrossRef]
21. Hsieh, Y.; Moo, C.; Liu, S.; Chang, Y. Distributive Maximum Power Point Tracking for Serial Photovoltaic Panels with Partial Power Regulation. In Proceedings of the 2019 9th IEEE International Conference on Control System, Computing and Engineering (ICCSCE), Penang, Malaysia, 29 November–1 December 2019.

22. Hong, Y.; Pham, S.N.; Yoo, T.; Chae, K.; Baek, K. Efficient Maximum Power Point Tracking for a Distributed PV System under Rapidly Changing Environmental Conditions. *IEEE Trans. Power Electron.* **2015**, *30*, 4209–4218. [CrossRef]

23. Ge, Z.; Li, X.; Xu, F.; Wu, H.; Wang, R.; Ding, S. An Improved Distributed Maximum Power Point Tracking Technique in Photovoltaic Systems Based on Reinforcement Learning Algorithm. *IEEE J. Emerg. Sel. Topics Ind. Electron.* **2024**, *5*, 167–178. [CrossRef]

24. Crăciun, B.; Kerekes, T.; Séra, D.; Teodorescu, R. Frequency Support Functions in Large PV Power Plants with Active Power Reserves. *IEEE J. Emerg. Sel. Topics Power Electron.* **2014**, *2*, 849–858. [CrossRef]

25. Mahmood, H.; Michaelson, D.; Jiang, J. Decentralized Power Management of a PV/Battery Hybrid Unit in a Droop-Controlled Islanded Microgrid. *IEEE Trans. Power Electron.* **2015**, *30*, 7215–7229. [CrossRef]

26. Vilathgamuwa, M.; Nayanasiri, D.; Gamini, S. *Power Electronic for Photovoltaic Power Systems*, 1st ed.; Springer Nature: Cham, Switzerland, 2015; pp. 22–30. ISBN 978-3-031-02500-6.

27. Sunny, A.C.; Debnath, D. A Novel Three-Port High-Gain DC–DC Converter for PV–Battery Stand-Alone System with Reduced Device Count. *IEEE J. Emerg. Sel. Topics Ind. Electron.* **2024**, *5*, 1216–1225. [CrossRef]

28. Ravada, B.R.; Tummuru, N.R. Control of a Supercapacitor-Battery-PV Based Stand-Alone DC-Microgrid. *IEEE Trans. Energy Convers.* **2020**, *35*, 1268–1277.

29. Joung, K.W.; Kim, T.; Park, J. Decoupled Frequency and Voltage Control for Stand-Alone Microgrid with High Renewable Penetration. *IEEE Trans. Ind. Appl.* **2019**, *55*, 122–133. [CrossRef]

30. Karimi, Y.; Oraee, H.; Guerrero, J.M. Decentralized Method for Load Sharing and Power Management in a Hybrid Single/Three-Phase-Islanded Microgrid Consisting of Hybrid Source PV/Battery Unit. *IEEE Trans. Power Electron.* **2017**, *32*, 6135–6144. [CrossRef]

31. Shafiullah, M.; Ahmed, S.; Al-sulaiman, F.A. Grid Integration Challenges and Solution Strategies for Solar PV Systems: A Review. *IEEE Access* **2022**, *10*, 52233–52257.

32. Behera, M.K.; Saikia, L.C. A Seamless Control of Grid-Connected PV System for Alleviating PV Penetration in Rural Grid Using Supercapacitor Accompanying with DSTATCOM and Improved CTF Control. *IEEE Trans. Ind. Appl.* **2024**, *60*, 3588–3602. [CrossRef]

33. Sekhar, K.S.R.; Chaudhari, M.A.; Khadkikar, V. Enhanced Hybrid Converter Topology for PV-Grid-EV Integration. *IEEE Trans. Energy Convers.* **2023**, *38*, 2634–2646. [CrossRef]

34. Yang, Y.; Blaabjerg, F.; Zou, Z. Benchmarking of Grid Fault Modes in Single-Phase Grid-Connected Photovoltaic Systems. *IEEE Trans. Ind. Appl.* **2013**, *49*, 2167–2176. [CrossRef]

35. Mohandes, B.; Moursi, M.S.E.; Hatziargyriou, N.; Khatib, S.E. A Review of Power System Flexibility with High Penetration of Renewables. *IEEE Trans. Power Syst.* **2019**, *34*, 3140–3155.

36. Fang, J.; Li, H.; Tang, Y.; Blaabjerg, F. On the Inertia of Future More-Electronics Power Systems. *IEEE J. Emerg. Sel. Top. Power Electron.* **2019**, *7*, 2130–2146. [CrossRef]

37. Cabrera-Tobar, A.; Bullich-Massagué, E.; Aragüés-Peñalba, M.; Gomis-Bellmunt, O. Active and reactive power control of a PV generator for grid code compliance. *Energies* **2019**, *12*, 3872. [CrossRef]

38. Zhang, Z.; Mishra, Y.; Dou, C.; Yue, D.; Zhang, B.; Tian, Y. Steady-State Voltage Regulation with Reduced Photovoltaic Power Curtailment. *IEEE J. Photovolt.* **2020**, *10*, 1853–1863. [CrossRef]

39. Tonkoski, R.; Lopes, L.A.C.; El-Fouly, T.H.M. Coordinated Active Power Curtailment of Grid Connected PV Inverters for Overvoltage Prevention. *IEEE Trans. Sustain. Energy.* **2011**, *2*, 139–147. [CrossRef]

40. Li, X.; Wen, H.; Zhu, Y.; Jiang, L.; Hu, Y.; Xiao, W. A Novel Sensorless Photovoltaic Power Reserve Control with Simple Real-Time MPP Estimation. *IEEE Trans. Power Electron.* **2019**, *34*, 7521–7531. [CrossRef]

41. Riquelme-Dominguez, J.M.; Martinez, S. A Photovoltaic Power Curtailment Method for Operation on Both Sides of the Power-Voltage Curve. *Energies* **2020**, *13*, 3906. [CrossRef]

42. Batzelis, E.I.; Kampitsis, G.E.; Papathanassiou, S.A. Power Reserves Control for PV Systems with Real-Time MPP Estimation via Curve Fitting. *IEEE Trans. Sustain. Energy* **2017**, *8*, 1269–1280. [CrossRef]

43. Sangwongwanich, A.; Yang, Y.; Blaabjerg, F.; Sera, D. Delta Power Control Strategy for Multistring Grid-Connected PV Inverters. *IEEE Trans. Ind. Appl.* **2017**, *53*, 3862–3870. [CrossRef]

44. Hoke, A.F.; Shirazi, M.; Chakraborty, S.; Muljadi, E.; Maksimovic, D. Rapid Active Power Control of Photovoltaic Systems for Grid Frequency Support. *IEEE J. Emerg. Sel. Top. Power Electron.* **2017**, *5*, 1154–1163. [CrossRef]

45. Ye, D.; Riquelme-Dominguez, J.M.; Martinez, S. Estimation of the Output Characteristic of a Photovoltaic Generator under Power Curtailment and Considering Converter Losses. *Electronics* **2022**, *11*, 1544. [CrossRef]

46. Hill, C.A.; Such, M.C.; Chen, D.; Gonzalez, J.; Grady, W.M. Battery Energy Storage for Enabling Integration of Distributed Solar Power Generation. *IEEE Trans. Smart Grid* **2012**, *3*, 850–857. [CrossRef]

47. Li, X.; Hui, D.; Lai, X. Battery Energy Storage Station (BESS)-Based Smoothing Control of Photovoltaic (PV) and Wind Power Generation Fluctuations. *IEEE Trans. Sustain. Energy* **2013**, *4*, 464–473. [CrossRef]

48. Zhang, H.; Zhai, X.; Zhang, J.; Bai, X.; Li, Z. Mechanism Analysis of the Effect of the Equivalent Proportional Coefficient of Inertia Control for a Doubly Fed Wind Generator on Frequency Stability in Extreme Environments. *Sustainability* **2024**, *16*, 4965. [CrossRef]

49. Abdollahy, S.; Mammoli, A.; Cheng, F.; Ellis, A.; Johnson, J. Distributed Compensation of a Large Intermittent Energy Resource in a Distribution Feeder. In Proceedings of the 2013 IEEE PES Innovative Smart Grid Technologies Conference (ISGT), Washington, DC, USA, 24–27 February 2013.

50. Ma, W.; Wang, W.; Wu, X.; Hu, R.; Tang, F.; Zhang, W.; Han, X.; Ding, L. Optimal Allocation of Hybrid Energy Storage Systems for Smoothing Photovoltaic Power Fluctuations Considering the Active Power Curtailment of Photovoltaic. *IEEE Access* **2019**, *7*, 1109. [CrossRef]

51. Ellis, A.; Schoenwald, D.; Hawkins, J.; Willard, S.; Arellano, B. PV Output Smoothing with Energy Storage. In Proceedings of the 2012 38th IEEE Photovoltaic Specialists Conference, Austin, TX, USA, 3–8 June 2012.

52. Abdalla, A.A.; Moursi, M.S.E.; El-Fouly, T.H.M.; Hosani, K.H.A. Reliant Monotonic Charging Controllers for Parallel-Connected Battery Storage Units to Reduce PV Power Ramp Rate and Battery Aging. *IEEE Trans. Smart Grid* **2023**, *14*, 4424–4438. [CrossRef]

53. Tran, V.T.; Islam, M.R.; Muttaqi, K.M.; Sutanto, D. A Novel Application of Magnesium Di-Boride Superconducting Energy Storage to Mitigate the Power Fluctuations of Single-Phase PV Systems. *IEEE Trans. Appl. Supercond.* **2019**, *29*, 5700505. [CrossRef]

54. Hossain, M.K.; Ali, M.H. Small scale energy storage for power fluctuation minimization with spatially diverged PV plants. In Proceedings of the 2013 Proceedings of IEEE Southeastcon, Jacksonville, FL, USA, 4–7 April 2013.

55. Alam, M.J.E.; Muttaqi, K.M.; Sutanto, D. Battery Energy Storage to Mitigate Rapid Voltage/Power Fluctuations in Power Grids Due to Fast Variations of Solar/Wind Outputs. *IEEE Access* **2021**, *10*, 1109. [CrossRef]

56. Kakimoto, N.; Satoh, H.; Takayama, S.; Nakamura, K. Ramp-Rate Control of Photovoltaic Generator with Electric Double-Layer Capacitor. *IEEE Trans. Energy Convers.* **2009**, *24*, 465–473. [CrossRef]

57. Alam, M.J.E.; Satoh, H.; Takayama, S.; Nakamura, K. A Novel Approach for Ramp-Rate Control of Solar PV Using Energy Storage to Mitigate Output Fluctuations Caused by Cloud Passing. *IEEE Trans. Energy Convers.* **2014**, *29*, 507–518.

58. Li, H.; Wei, H. High Voltage Ride-Through Control Strategy for Two-Stage PV Grid-Connected Systems. In Proceedings of the 2023 2nd Asia Power and Electrical Technology Conference (APET), Shanghai, China, 28–30 December 2023.

59. Zhang, N.; Sutanto, D.; Muttaqi, K.M. A review of topologies of three-port DC-DC converters for the integration of renewable energy and energy storage system. *Renew. Sustain. Energy Rev.* **2016**, *56*, 388–401. [CrossRef]

60. Wang, G.; Wen, H.; Xu, P.; Liu, W.; Zhou, J.; Yang, Y. A Comprehensive Review of Integrated Three-Port DC-DC Converters with Key Performance Indices. *IEEE Trans. Power Electron.* **2024**, *39*, 6391–6408. [CrossRef]

61. Elmakawi, A.; Bayındır, K. High-Gain Non-Isolated Three-Port Converter for Building-Integrated PV Systems. *Electronics* **2022**, *11*, 387. [CrossRef]

62. Jiang, Y.; Liu, F.; Ruan, X.; Wang, L. Optimal idling control strategy for three-port full-bridge converter. In Proceedings of the 2014 International Power Electronics Conference (IPEC-Hiroshima 2014—ECCE ASIA), Hiroshima, Japan, 18–21 May 2014.

63. Wang, L.; Wang, Z.; Li, H. Asymmetrical Duty Cycle Control and Decoupled Power Flow Design of a Three-port Bidirectional DC-DC Converter for Fuel Cell Vehicle Application. *IEEE Trans. Power Electron.* **2011**, *27*, 891–904. [CrossRef]

64. Phattanasak, M.; Gavagsaz-Ghoachani, R.; Martin, J.; Nahid-Mobarakeh, B.; Pierfederici, S.; Davat, B. Control of a Hybrid Energy Source Comprising a Fuel Cell and Two Storage Devices Using Isolated Three-Port Bidirectional DC-DC Converters. *IEEE Trans. Ind. Appl.* **2015**, *51*, 491–497. [CrossRef]

65. Liu, D.; Li, H. A ZVS Bi-Directional DC-DC Converter for Multiple Energy Storage Elements. *IEEE Trans. Power Electron.* **2006**, *21*, 1513–1517. [CrossRef]

66. Hu, W.; Wu, H.; Xing, Y.; Sun, K. A full-bridge three-port converter for renewable energy application. In Proceedings of the 2014 IEEE Applied Power Electronics Conference and Exposition—APEC 2014, Fort Worth, TX, USA, 16–20 March 2014.

67. Chen, Z. Three-port ZVS converter with PWM plus secondary-side phase-shifted for photovoltaic-storage hybrid systems. In Proceedings of the 2014 IEEE Applied Power Electronics Conference and Exposition—APEC 2014, Fort Worth, TX, USA, 16–20 March 2014.

68. Hu, Y.; Xiao, W.; Gao, W.; Ji, B.; Morrow, D. Three-Port DC-DC Converter for Stand-Alone Photovoltaic Systems. *IEEE Trans. Power Electron.* **2014**, *30*, 3068–3076. [CrossRef]

69. Zhu, H.; Zhang, D.; Athab, H.; Wu, B.; Gu, Y. PV Isolated Three-Port Converter and Energy-Balancing Control Method for PV-Battery Power Supply Applications. *IEEE Trans. Ind. Electron.* **2015**, *62*, 3595–3606. [CrossRef]

70. Taheri, S.M.; Baghramian, A.; Pourseyedi, S.A. A Novel High-Step-Up SEPIC-Based Nonisolated Three-Port DC–DC Converter Proper for Renewable Energy Applications. *IEEE Trans. Power Electron.* **2023**, *70*, 10114–10122. [CrossRef]

71. Zhang, Y.; Li, S.; Wang, Y.; Wang, J.; Chen, Z.; Huang, Y. A Two-Switch SEPIC-Based Nonisolated Three-Port Converter Featuring High Step-Up Gain for Solar PV Applications. *Electronics* **2023**, *12*, 1712. [CrossRef]

72. Cheng, T.; Lu, D.D.C.; Qin, L. Non-Isolated Single-Inductor DC/DC Converter with Fully Reconfigurable Structure for Renewable Energy Applications. *IEEE Trans. Circuits Syst. II Express Briefs* **2018**, *65*, 351–355. [CrossRef]

73. Moradisizkoohi, H.; Elsayad, N.; Mohammed, O.A. A Family of Three-Port Three-Level Converter Based on Asymmetrical Bidirectional Half-Bridge Topology for Fuel Cell Electric Vehicle Applications. *IEEE Trans. Power Electron.* **2019**, *34*, 11706–11724. [CrossRef]

74. Nair, S.S.; Rajeev, M. A Novel High Gain Non-Isolated Three-port Converter for Stand-Alone PV Applications. In Proceedings of the 2023 International Conference on Computer, Electronics & Electrical Engineering & their Applications (IC2E3), Srinagar Garhwal, India, 8–9 June 2023.

75. Liang, T.-J.; Tran, T.A.A.; Huynh, K.K.N.; Chen, K.-H. Soft-Switching Three-Port Converter with a Three-Winding Coupled Inductor. *IEEE J. Emerg. Sel. Top. Power Electron.* **2023**, *11*, 5470–5485. [CrossRef]

76. Qin, S.; Lei, Y.; Barth, C.; Liu, W.; Pilawa-Podgurski, R.C.N. A High Power Density Series-Stacked Energy Buffer for Power Pulsation Decoupling in Single-Phase Converters. *IEEE Trans. Power Electron.* **2017**, *32*, 4905–4924. [CrossRef]

77. Iyer, V.M.; Gulur, S.; Gohil, G.; Bhattacharya, S. An Approach Towards Extreme Fast Charging Station Power Delivery for Electric Vehicles with Partial Power Processing. *IEEE Trans. Ind. Electron.* **2020**, *67*, 8076–8087. [CrossRef]

78. Pape, M.; Kazerani, M. An Offshore Wind Farm with DC Collection System Featuring Differential Power Processing. *IEEE Trans. Energy Convers.* **2020**, *35*, 222–236. [CrossRef]

79. Zapata, J.W.; Kouro, S.; Carrasco, G.; Renaudineau, H.; Meynard, T.A. Analysis of Partial Power DC-DC Converters for Two-Stage Photovoltaic Systems. *IEEE J. Emerg. Sel. Top. Power Electron.* **2019**, *7*, 591–603. [CrossRef]

80. Zapata, J.W.; Kouro, S.; Carrasco, G.; Meynard, T.A. Step-Down Partial Power DC-DC Converters for Two-Stage Photovoltaic String Inverters. *Electronics* **2019**, *8*, 87. [CrossRef]

81. Moo, C.S.; Chen, Y.J.; Yan, W.Q. An Efficient Driver for Dimmable LED Lighting. *IEEE Trans. Power Electron.* **2012**, *27*, 4613–4618. [CrossRef]

82. Hassanpour, N.; Chub, A.; Blinov, A.; Vinnikov, D. Soft-Switching Bidirectional Step-Up/Down Partial Power Converter with Reduced Components Stress. *IEEE Trans. Power Electron.* **2023**, *38*, 14166–14177. [CrossRef]

83. Artal-Sevil, J.S.; Anzola, J.; Ballestín-Bernad, V.; Bernal-Agustín, J.L. Analysis and Implementation of different non-isolated Partial-Power Processing Architectures based on the Cuk Converter. In Proceedings of the 2022 24th European Conference on Power Electronics and Applications (EPE'22 ECCE Europe), Hanover, Germany, 5–9 September 2022.

84. Xu, R.; Gao, S.; Wang, Y.; Xu, D. A High Step Up SEPIC-Based Partial-Power Converter with wide input range. In Proceedings of the 2021 IEEE Industry Applications Society Annual Meeting (IAS), Vancouver, BC, Canada, 10–14 October 2021.

85. Chen, L.; Wu, H.; Xu, P.; Hu, H.; Wan, C. A high step-down non-isolated bus converter with partial power conversion based on synchronous LLC resonant converter. In Proceedings of the 2015 IEEE Applied Power Electronics Conference and Exposition (APEC), Charlotte, NC, USA, 15–19 March 2015.

86. Lai, J.; Peng, H.; Hu, J.; Huang, S.; Wang, W. Partial Power Processing DC Current Source for The Loop Resistance Measurement in Gas Insulated Switchgear. In Proceedings of the 2018 International Conference on Power System Technology (POWERCON), Guangzhou, China, 6–8 November 2018.

87. Jiang, J.; Zhang, T.; Chen, D. Analysis, Design, and Implementation of a Differential Power Processing DMPPT With Multiple Buck–Boost Choppers for Photovoltaic Module. *IEEE Trans. Power Electron.* **2021**, *36*, 10214–10223. [CrossRef]

88. Kjaer, S.B.; Pedersen, J.K.; Blaabjerg, F. A Review of Single-Phase Grid-Connected Inverters for Photovoltaic Modules. *IEEE Trans. Ind. Appl.* **2005**, *41*, 1292–1306. [CrossRef]

89. Zhou, H.; Zhao, J.; Han, Y. PV Balancers: Concept, Architectures, and Realization. *IEEE Trans. Power Electron.* **2015**, *30*, 3479–3487. [CrossRef]

90. Nimni, Y.; Shmilovitz, D. A Returned Energy Architecture for Improved Photovoltaic Systems Efficiency. In Proceedings of the 2010 IEEE International Symposium on Circuits and Systems, Paris, France, 30 May–2 June 2010.

91. Sun, X.; He, X.; Wang, H.; Wang, F.; Zhuo, F.; Yi, H. Analysis and Comparison of Partial Power Processing Based DC-DC Converters in Renewable Energy Application. In Proceedings of the 2018 IEEE International Power Electronics and Application Conference and Exposition (PEAC), Shenzhen, China, 4–7 November 2018.

92. Qin, S.; Morrison, A.J.; Pilawa-Podgurski, R.C.N. Enhancing Micro-inverter Energy Capture with Sub-module Differential Power Processing. In Proceedings of the 2014 IEEE Applied Power Electronics Conference and Exposition—APEC 2014, Fort Worth, TX, USA, 16–20 March 2014.

93. Müller, N.; Kouro, S.; Zanchetta, P.; Wheeler, P. Bidirectional Partial Power Converter Interface for Energy Storage Systems to Provide Peak Shaving in Grid-Tied PV Plants. In Proceedings of the 2018 IEEE International Conference on Industrial Technology (ICIT), Lyon, France, 20–22 February 2018.

94. Shenoy, P.S.; Kim, K.A.; Krein, P.T. Comparative Analysis of Differential Power Conversion Architectures and Controls for Solar Photovoltaics. In Proceedings of the 2012 IEEE 13th Workshop on Control and Modeling for Power Electronics (COMPEL), Kyoto, Japan, 10–13 June 2012.

95. Lee, H.; Kim, K.A. Design Considerations for Parallel Differential Power Processing Converters in a Photovoltaic-Powered Wearable Application. *Energies* **2018**, *11*, 3329. [CrossRef]

96. Uno, M.; Shinohara, T. Module-Integrated Converter Based on Cascaded Quasi-Z-Source Inverter with Differential Power Processing Capability for Photovoltaic Panels Under Partial Shading. *IEEE Trans. Power Electron.* **2019**, *34*, 11553–11565. [CrossRef]

97. Uno, M.; Yamamoto, M.; Sato, H.; Oyama, S. Modularized Differential Power Processing Architecture Based on Switched Capacitor Converter to Virtually Unify Mismatched Photovoltaic Panel Characteristics. *IEEE Trans. Power Electron.* **2020**, *35*, 1563–1575. [CrossRef]

98. Villa, L.F.L.; Ho, T.; Crebier, J.; Raison, B. A Power Electronics Equalizer Application for Partially Shaded Photovoltaic Modules. *IEEE Trans. Power Electron.* **2013**, *60*, 1179–1190.

99. Liu, C.; Zheng, Y.; Lehman, B. PV Panel to PV Panel Transfer Method for Modular Differential Power Processing. *IEEE Trans. Power Electron.* **2022**, *37*, 4764–4778. [CrossRef]

100. Jeong, H.; Lee, H.; Liu, Y.; Kim, K.A. Review of Differential Power Processing Converter Techniques for Photovoltaic Applications. *IEEE Trans. Energy Convers.* **2019**, *34*, 351–360. [CrossRef]

101. Chu, G.; Wen, H.; Jiang, L.; Hu, Y.; Li, X. Bidirectional flyback based isolated-port submodule differential power processing optimizer for photovoltaic applications. *Sol. Energy* **2017**, *158*, 929–940. [CrossRef]

102. Alenezi, A.; Hussain, H. A New Control Approach for Least Processed Power Tracking Under Mismatch Conditions in PV Systems Using Differential Power Processing. *IEEE Trans. Ind. Appl.* **2024**, *60*, 532–543. [CrossRef]

103. Wang, X.; Wen, H.; Chu, G.; Zhu, Y.; Yang, Y.; Wang, Y.; Jiang, L. Performance Quantization and Comparative Assessment of Voltage Equalizers in Mismatched Photovoltaic Differential Power Processing Systems. *IEEE Trans. Power Electron.* **2024**, *39*, 1656–1675. [CrossRef]